Benchmarking of simulation codes for high intensity hydrogen ion linacs *

J.-P. Carneiro
FNAL Accelerator Physics Department

March 8, 2007

Abstract

This document presents the benchmarking of two beam dynamics simulation codes, `TRACK` and `ASTRA`, with application to a FNAL superconducting 8-GeV hydrogen ion linac. `TRACK`, developed by Argonne National Laboratory to fulfill the requirement of heavy-ion linacs, is the primary tool in the design of the accelerator. `ASTRA`, developed by the Deutsches Elektronen-Synchrotron laboratory (Hamburg, Germany), is mainly used for the design of electron photo-injectors. We present for the first time the application of this code for hydrogen ions.

1 Introduction

Fermilab is developing the concept and design of a High Intensity Proton Source based on an 8 GeV superconducting H^- linac with the primary mission of increasing the intensity of the Fermilab Main Injector for the production of neutrino superbeams. Observation of CP violation, measurement of the neutrino mass-squared differences and general understanding of neutrino properties are goals of the U.S. neutrino programs this accelerator is designed to address. Figure 1 presents a layout of the linac.

*Beams-doc-2396. Also submitted to NIM A, Feb. 2007.

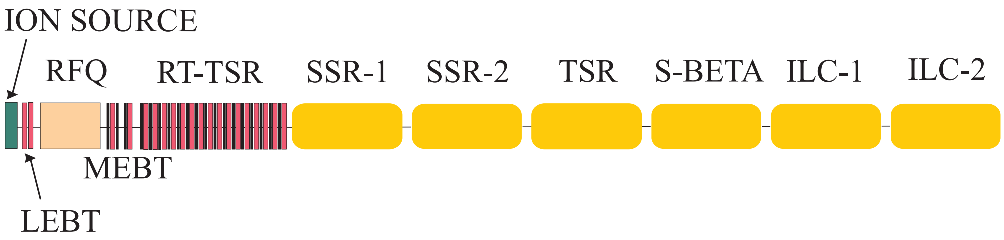

Figure 1: Layout of the Fermilab High Intensity Proton Source Linac.

The main elements of the accelerator are an H^- Ion Source, a Low Energy Beam Transport (LEBT) to match the beam into a Radio-Frequency Quadrupole (RFQ), a Medium Energy Beam Transport (MEBT) with 2 Room Temperature (RT) bunching cavities and a beam chopper followed by 16 RT Triple Spoke Resonators (RT-TSR), 18 superconducting Single Spoke Resonators of Type 1 (SSR1) and 33 longer ones (SSR2), 42 superconducting Triple Spoke Resonators (TSR), 56 Squeezed ILC-type superconducting cavities (S-ILC) designed for $\beta_G = 0.81$ and 287 ILC-type cavities. The transverse focusing up to the TSR section is achieved with 57 superconducting solenoids and with 117 normal conducting quadrupoles from the S-ILC section to the end of the linac. The ILC-type section is divided in 9 cryomodules containing 2 quadrupoles and 7 cavities (ILC1) followed by 28 cryomodules with 1 quadrupole and 8 cavities (ILC2). The length and output kinetic energy W_{out} of each section is presented in Table 1. A detailed description of the accelerator can be found in References [1] and [2].

Table 1: Linac main section lengths and output kinetic energy.

Section	**Length**	$\mathbf{W_{out}}$
Ion Source+LEBT	~0.2 m	50 keV
RFQ	~4.0 m	2.5 MeV
MEBT+RT-TSR	12.6 m	8.8 MeV
SSR1+SSR2	43.1 m	121 MeV
TSR	81.6 m	421 MeV
S-ILC	85.4 m	1.2 GeV
ILC1+ILC2	451.4 m	8 GeV

The accelerator is designed to deliver $1.56 \cdot 10^{14}$ protons to the FNAL Main Injector in typical pulse lengths of 1 msec leading to an average beam current of 25 mA per pulse. At a beam kinetic energy of 8 GeV and a repetition rate of 10 Hz the corresponding beam average power is ∼2 MW. An outstanding feature of this accelerator is the use of ferrite phase shifters [3] which allow a small number of klystrons to each power many cavities. In the baseline design, a single 325 MHz klystron is foreseen to power the front-end linac (from IS to TSR section), and 10 ILC-type klystrons operating at 1300 MHz are required for the remaining section of the accelerator.

2 Code description

2.1 Integration of the equations of motion

The equations of motion for a particle in an electromagnetic field are :

$$\frac{d\vec{r}}{dt} = \frac{\vec{p}}{m_0\gamma} \tag{1}$$

$$\frac{d\vec{p}}{dt} = q(\vec{E} + \frac{\vec{p}}{m_0\gamma} \times \vec{B}) \tag{2}$$

with $\vec{r}$ the particle coordinate, $\vec{p}$ the mechanical momentum, $\gamma = \sqrt{1-\beta^2}$, $\beta = v/c$, v and c particle and light speed, q and m_0 charge and rest mass of accelerated particle and $\vec{E}$ and $\vec{B}$ the electric and magnetic fields. Both codes `TRACK` [4] and `ASTRA` [5] perform the integration of Equations (1) and (2) by the Runge-Kutta method of forth order, with a variable integration step size for both codes. `TRACK` uses a spatial integration step defined for each element of the beam line while `ASTRA` uses a user defined temporal integration step. The fields $\vec{E}$ and $\vec{B}$ include external contribution from accelerating and focusing fields and internal from the beam space charge forces. Both codes have the ability of using 2D external electric fields defined on the cavity axis or 3D external electric fields defined on a rectangular mesh. Concerning the external solenoid magnetic fields, `TRACK` can handle both 2D or 3D fields while `ASTRA` supports only 2D ones. For the simulations presented in this document, both codes were provided with the exact 3D electric fields, in binary format for `TRACK` and ASCII for `ASTRA`, and with the exact 2D solenoid magnetic fields on axis in ASCII format. `TRACK` and `ASTRA` perform the same polynomial expansion to 3^{rd} order as :

$$B_z(z,r) = B_z(z,0) - \frac{r^2}{4}\left(\frac{d^2B}{dz^2} - \frac{d^4B}{dz^4}\frac{r^2}{16} + \frac{d^6B}{dz^6}\frac{r^4}{576}\right) \quad (3)$$

$$B_r(z,r) = -\frac{r}{2}\left(\frac{dB}{dz} - \frac{d^3B}{dz^3}\frac{r^2}{8} + \frac{d^5B}{dz^5}\frac{r^4}{192}\right) \quad (4)$$

with $B_{z,0}$ the longitudinal on-axis magnetic field.

For the simulations presented in this paper, the space-charge forces were computed using the 3D space charge calculation available in TRACK and ASTRA. For both codes, the space-charge fields are calculated in the beam rest frame via Poisson's equation :

$$\nabla^2\phi(r,\theta,z) = -\frac{\rho(r,\theta,z)}{\epsilon_0} \quad (5)$$

with ϕ the electrostatic potential, ρ the charge density, ϵ_0 the dielectric constant and Lorentz's transformed back into the laboratory frame. A 3D Cartesian grid is used for both codes with the calculation of the electrostatic potential at each grid point. On the boundaries, TRACK considers ideal parallel conducting walls transversely and free-space longitudinally while ASTRA solves Poisson's equation in free-space.

Finally, it is important to notice that, unlike TRACK, the code ASTRA does not handle the RFQ. Therefore, the codes benchmarking starts at the exit of this element.

2.2 Output parameters

TRACK and ASTRA both provide numerous beam output parameters. In this document we consider the following beam parameters: RMS transverse size σ_x and σ_y, RMS normalized transverse emittance ϵ_x and ϵ_y, RMS bunch length σ_z, RMS normalized longitudinal emittance ϵ_z, kinetic energy W and RMS energy spread σ_E. The ASTRA units for these parameters are taken as reference. The RMS normalized transverse emittance is defined in this document by the relation :

$$\epsilon_u = \beta\gamma\sqrt{\langle u^2\rangle\langle(u')^2\rangle - \langle uu'\rangle^2}; \quad (6)$$

with β and γ the parameters defined in the previous section, u and u' the transverse coordinate and divergence of x or y, and $\langle\rangle$ an RMS value.

Table 2: Initial beam parameters (at $z = 0$ m, RFQ exit).

Beam parameters	**Zero Current**	**43.25 mA**
RMS size σ_X	0.69 mm	0.74 mm
RMS size σ_Y	0.68 mm	0.72 mm
Norm. RMS emittance ϵ_X	0.25 mm-mrad	0.25 mm-mrad
Norm. RMS emittance ϵ_Y	0.26 mm-mrad	0.25 mm-mrad
RMS bunch length σ_Z	1.75 mm	1.85 mm
Norm. RMS emittance ϵ_Z	45.9 kev-mm	25.6 kev-mm
Kinetic Energy W	2.51 MeV	2.52 MeV
RMS energy spread σ_E	28.6 keV	17.8 keV

3 Methodology

This document presents benchmarking of TRACK and ASTRA from the exit of the RFQ up to the last accelerating section (ILC2), covering a length of $\sim$674 m. First the Zero Current case is considered for its simplicity. In this scenario, the benchmarking ignores the space charge effects, implying linear beam dynamics and fast simulations. Then the benchmarking is performed for a linac peak current of 43.25 mA. Reference [2] describes that in order to avoid beam losses during RF capture and to provide a gap for the extraction kicker in the Main Injector, a linac peak current of 43.25 mA is necessary to deliver the desired 25 mA average macropulse current to the Main Injector.

Beam dynamics simulation in the RFQ has been performed with TRACK as presented in Reference [6]. This provides, at the RFQ exit, two particle distributions of $1{\cdot}10^4$ and $2{\cdot}10^5$ particles respectively for the Zero Current and the 43.25 mA cases. Table 2 shows the beam parameters of each initial distribution as provided as inputs to TRACK and ASTRA.

4 Code Benchmarking

4.1 Zero Current

Figure 2 presents TRACK and ASTRA Zero Current simulations of the High Intensity Proton Source Linac, from the RFQ exit to the last ILC2 cryomodule. The final beam param-

Table 3: TRACK and ASTRA outputs for Zero Current (at $z \simeq 674$ m).

Beam parameters	**TRACK**	**ASTRA**
RMS size σ_X	1.71 mm	1.88 mm
RMS size σ_Y	0.98 mm	0.97 mm
Norm. RMS emit. ϵ_X	0.263 mm-mrad	0.265 mm-mrad
Norm. RMS emit. ϵ_Y	0.258 mm-mrad	0.260 mm-mrad
RMS bunch length σ_Z	0.251 mm	0.256 mm
Norm. RMS emit. ϵ_Z	643 kev-mm	648.2 kev-mm
Kinetic Energy W	7971 MeV	7973 MeV
RMS energy spread σ_E	2630 keV	2565 keV

eters from both codes are presented in Table 3.

An overall excellent agreement between the simulation codes TRACK and ASTRA for the Zero Current case is seen in Figure 2 and Table 3. The longitudinal parameters (RMS bunch length, RMS normalized longitudinal emittance, kinetic energy and RMS energy spread) are within 3% between the simulation codes at the end of the linac, after ∼674 meters of simulations. The transverse RMS size of the beam differs between the codes by ∼10% horizontally and by ∼1% vertically. Also a slight difference in the RMS transverse emittance between TRACK and ASTRA can be observed in Figure 2(b), the transverse emittances from ASTRA being slightly higher (∼0.7% horizontally and vertically) than those from TRACK. A possible explanation for this difference is the different step size used by the codes for the integration of the equations of motion (1) and (2) by the Runge-Kunta method of fourth order.

The impact of the integration step size on the beam dynamics simulation is presented in Figure 3. It shows the RMS transverse size and RMS normalized transverse emittance for the ILC1+ILC2 section (total length of ∼451.4 meters, see Table 1) at Zero Current using four different integration time steps: 10 ps, 50 ps, 100 ps and 150 ps. This figure confirms that the accuracy of the simulation depends on the integration step size, the smaller the time step the higher the accuracy.

Defining the same integration step size for both codes is not realistic. TRACK uses a spatial step size defined for each beam line element. ASTRA uses a temporal step which was defined at Zero Current between 60 ps and 150 ps as a trade-off between accuracy and CPU time. Therefore, this difference in the integration step size between the codes will ineluctably lead to a discrepancy between the output parameters, as presented in Table 3.

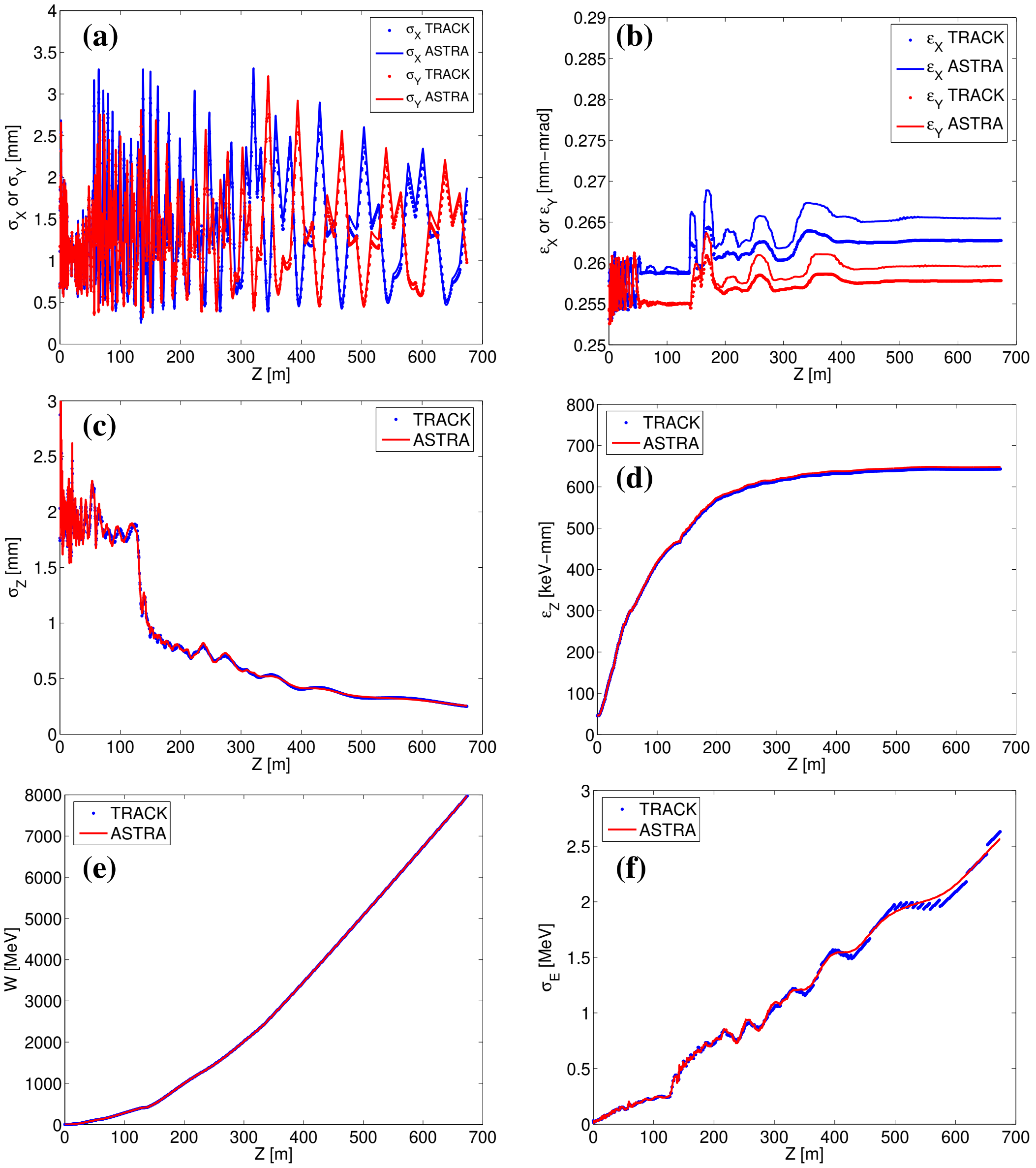

Figure 2: TRACK and ASTRA simulations of the High-Intensity Proton Source with Zero Current, from the RFQ exit ($z = 0$ m) to the last accelerating cavity ($z \simeq 674$ m) . From top left to bottom right: (a) RMS transverse size, (b) RMS normalized transverse emittance, (c) RMS bunch length, (d) RMS normalized longitudinal emittance, (e) kinetic energy and (f) RMS energy spread.

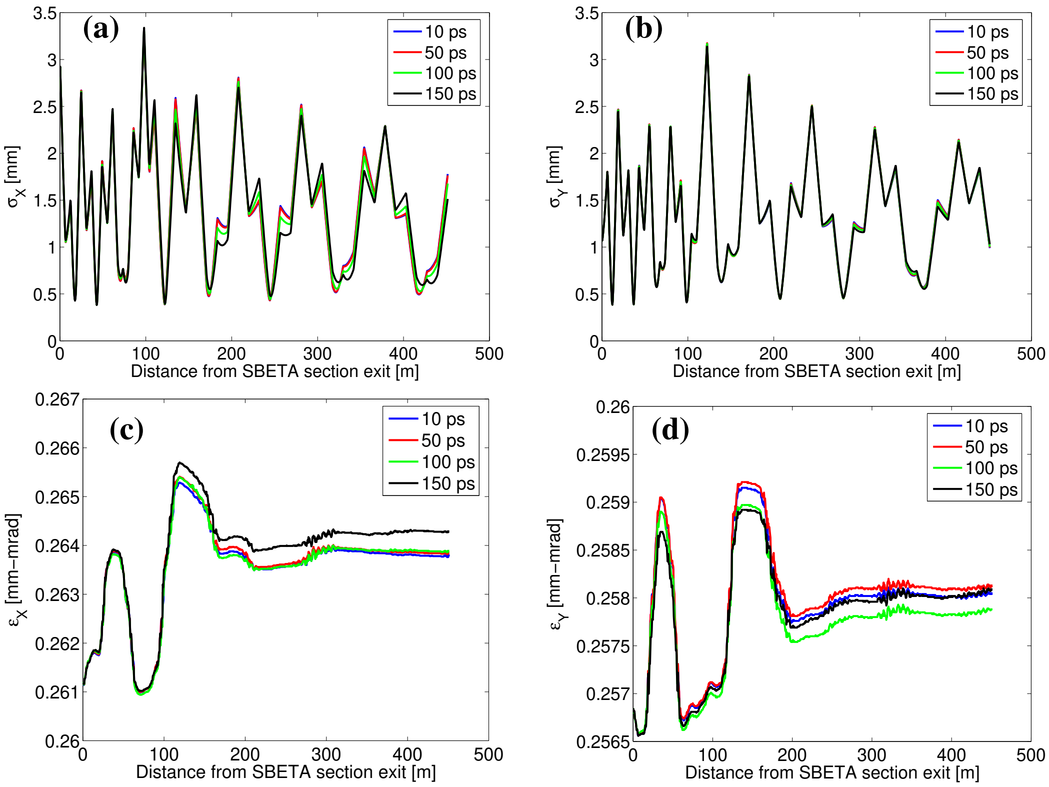

Figure 3: ASTRA simulations of the ILC1+ILC2 section of the High Intensity Proton Source (total length ∼451.4 m), at Zero Current and four different integration time steps: 10 ps, 50 ps, 100 ps and 150 ps. From top left to bottom right: (a) RMS horizontal size, (b) RMS vertical size, (c) RMS horizontal emittance, (d) RMS vertical emittance.

4.2 3D Uniform Ellipsoidal Bunch

As an intermediate step towards the code benchmarking at high peak current, the transverse and longitudinal on-axis space charge fields of an ideal 3D uniform ellipsoidal bunch were calculated by the 3D space routines of both `TRACK` and `ASTRA` and compared with the analytical expressions. 3D uniform ellipsoidal distributions represent the only distribution whose space charge field can be calculated analytically. Inside the ellipsoid the space-charge fields are a linear function of the position and can be expressed in the bunch rest frame by [7]:

$$\begin{aligned}
E_x^{sc} &= \frac{I\lambda(1-f)}{4\pi\epsilon_0 c(r_x+r_y)r_z}\cdot\frac{x}{r_x} \qquad x \le r_x \qquad (7)\\
E_y^{sc} &= \frac{I\lambda(1-f)}{4\pi\epsilon_0 c(r_x+r_y)r_z}\cdot\frac{y}{r_y} \qquad y \le r_y \qquad (8)\\
E_z^{sc} &= \frac{I\lambda f}{4\pi\epsilon_0 c r_x r_y}\cdot\frac{z}{r_z} \qquad z \le r_z \qquad (9)
\end{aligned}$$

with I the average current over an RF period, λ the RF wavelength, f a geometrical form factor, ϵ_0 the permittivity of free space r_x, r_y and r_z are the semi-axes of the ellipse in the laboratory frame which are related to the RMS beams sizes σ_x, σ_y and σ_z by $r_x = \sqrt{5}\cdot\sigma_x$, $r_y = \sqrt{5}\cdot\sigma_y$ and $r_z = \sqrt{5}\cdot\sigma_z$.

For ellipsoidal distributions of equal transverse sizes ($r_x = r_y$) the form factor f depends on the parameter $p = \gamma r_z/\sqrt{r_x r_y}$ with γ the Lorentz factor and satisfies [8]:

$$f = \int_0^1 \frac{\nu^2 d\nu}{\left[p^2+(1-p^2)\nu^2\right]^2} \qquad (10)$$

The space charge fields outside the ellipsoid are given also by Equations (7)-(9) with $r_x = \sqrt{r_x^2+\chi}$, $r_y = \sqrt{r_y^2+\chi}$ and $r_z = \sqrt{r_z^2+\chi}$ where the external point $\chi(x,y,z)$ is the positive root of the Equation :

$$\frac{x^2}{r_x^2+\chi}+\frac{y^2}{r_y^2+\chi}+\frac{z^2}{r_z^2+\chi} = 1 \qquad (11)$$

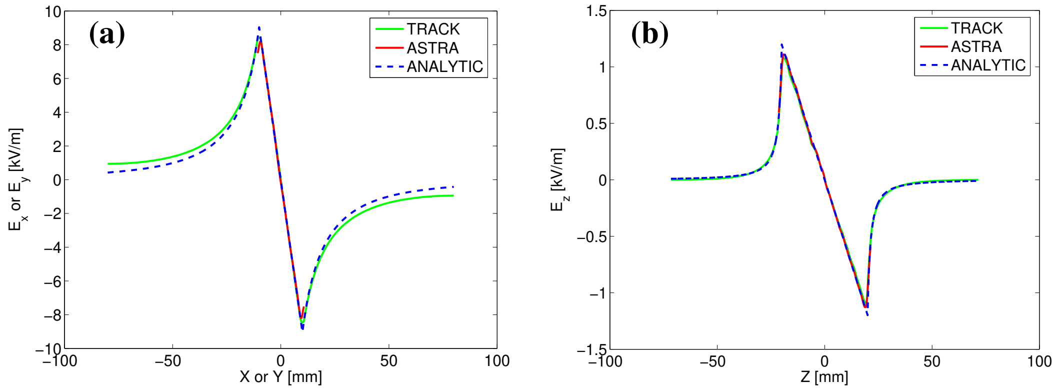

Figure 4: (a) Transverse and (b) Longitudinal electric field of an uniform ellipsoidal bunch from TRACK, ASTRA and analytical method.

Figure 4 shows the comparison between the analytical space charge fields and those from TRACK and ASTRA on the transverse and longitudinal axis of a 3D uniform ellipsoid filled with $2{\cdot}10^5$ particles of unit charge (with semi-axis length of 1 cm transversely and 2 cm longitudinally). On the longitudinal axis, the agreement is excellent. On the transverse axis, the space charge field outside the bunch provided by TRACK slightly differs from that computed from the analytical expressions. As mentioned in Section 2.1, TRACK computes the space charge fields taking into account the image charge of the beam on the conducting wall surface. Reference [9] mentions that the image charge increases the radial defocussing space charge fields, which explains the difference observed in Figure 4(a). Using a sufficiently high number of macro-particles and properly setting up the space charge grids, TRACK and ASTRA provide similar space charge fields for similar input distributions.

4.3 43.25 mA

Figure 5 presents TRACK and ASTRA simulations of the High Intensity Proton Source Linac, from the RFQ exit to the last ILC2 cyomodule for a linac peak current of 43.25 mA. The final beam parameters of both codes are presented in Table 4.

For space charge calculations, a grid of $64\times64\times64$ was implemented into ASTRA and an adjustable grid of $65\times65\times129$ for the first two cavities, $65\times65\times65$ in the SC Single-Spoke Resonator section and $129\times129\times65$ beyond into TRACK. Figure 5 and Table 4 report that the transverse beam dynamics agree within 10% between both codes. As pre-

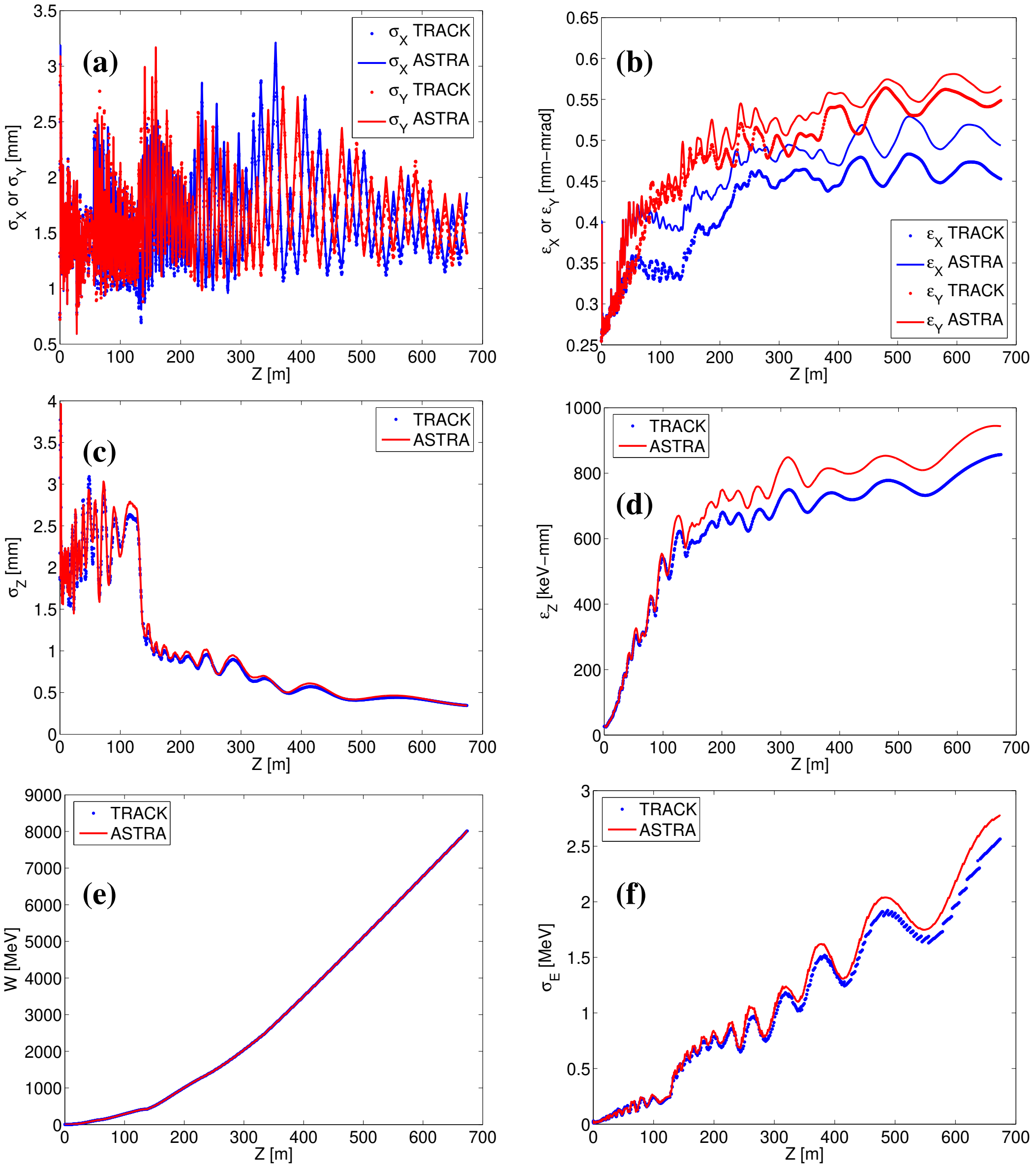

Figure 5: `TRACK` and `ASTRA` simulations of the High-Intensity Proton Source for a linac peak current of 43.25 mA, from the RFQ exit ($z = 0$ m) to the last accelerating cavity ($z \simeq 674$ m). From top left to bottom right: (a) RMS transverse size, (b) RMS normalized transverse emittance, (c) RMS bunch length, (d) RMS normalized longitudinal emittance, (e) kinetic energy and (f) RMS energy spread.

Table 4: TRACK and ASTRA outputs for 43.25 mA (at $z \simeq 674$ m).

Beam parameters	**TRACK**	**ASTRA**
RMS size σ_X	1.76 mm	1.87 mm
RMS size σ_Y	1.32 mm	1.34 mm
Norm. RMS emit. ϵ_X	0.458 mm-mrad	0.493 mm-mrad
Norm. RMS emit. ϵ_Y	0.549 mm-mrad	0.566 mm-mrad
RMS bunch length σ_Z	0.345 mm	0.3451 mm
Norm. RMS emit. ϵ_Z	857 kev-mm	943 kev-mm
Kinetic Energy W	8013 MeV	8009 MeV
RMS energy spread σ_E	2564 keV	2773 keV

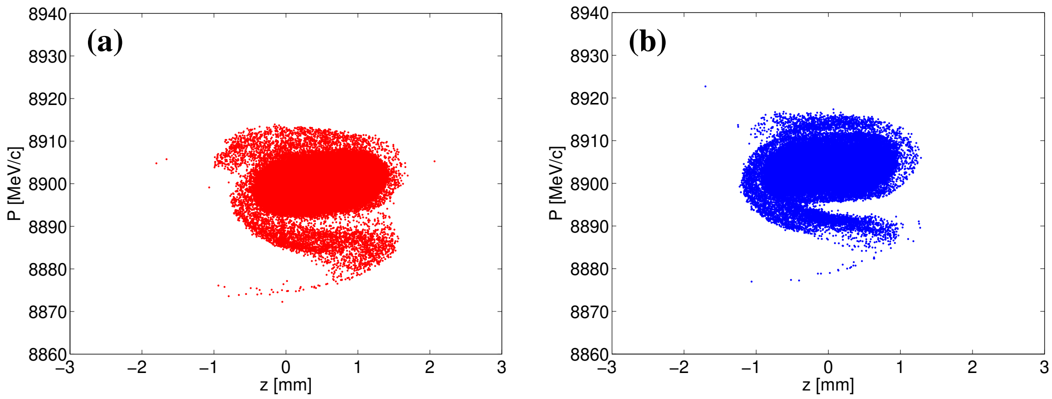

Figure 6: (a) TRACK and (b) ASTRA longitudinal phase space at the last accelerating cavity ($z \simeq 674$ m) of the High-Intensity Proton Source for a linac peak current of 43.25 mA.

viously described, integration step size might explain this disagreement. In contrast to the Zero Current case, some disagreement in longitudinal beam dynamics is observed starting from the S-ILC section (~137 m). This disagreement is more pronounced for the longitudinal emittance and energy spread than for the bunch length but stays within ~10% between both codes. Figure 6 presents the longitudinal phase space from TRACK and ASTRA at $z \simeq 674$ m and confirms the good agreement between both simulation codes.

5 Conclusion

A benchmarking of the simulation codes `TRACK` and `ASTRA` has been presented with an application to the FNAL superconducting H^- linac. The simulations were performed on an overal length of ∼674 meters (including 454 cavities, 117 quadrupoles and 55 solenoids), with an energy ranging from ∼2.5 MeV to ∼8 GeV and for two operating currents: Zero Current (space charge off) and 43.25 mA peak (using 3D space charge routine). Agreement to within 10% was found between the codes for both the transverse and longitudinal parameters. A preliminary report of this work was presented in [10]. The simulations presented on this paper use more accurate 3D electric fields and 2D magnetic fields. This paper also emphasizes the impact of the integration step size on the beam dynamics and the effect of the image charge on the space charge fields.

Acknowledgments

The author would like to thank P. Ostroumov and V. Aseev (ANL) for helpful discussions about `TRACK`, K. Floettmann (DESY) for his support in using `ASTRA`, and B. Webber and V. Shiltsev (FNAL) for their encouragement.

References

[1] G.W. Foster (Editor), *An 8-GeV Superconducting Linac Proton Driver*, available at : http://protondriver.fnal.gov/SCRF_PD_v56.doc

[2] P.N. Ostroumov, *Physics design of the 8-GeV H-minus Linac* , New Journal of Physics, **8**, 281 (2006).

[3] R. Madrak et al.,*New Materials and Designs for High-Power, Fast, Phase Shifters*, Proceedings of Linear Accelerator Conference, Knoxville, Tennessee (2006).

[4] V.N. Aseev, P.N. Ostroumov, E.S. Lessner and B. Mustapha, *TRACK : The new beam dynamics code*, Proceedings of Particle Accelerator Conference, Knoxville, Tennessee (2005).

[5] K. Flöttmann, ASTRA user manual available at :
http://www.desy.de/˜mpyflo/Astra_dokumentation/

[6] P.N. Ostroumov, V.N. Aseev and A.A. Kolomiets, *Application of a new procedure for design of 325 MHz RFQ*, Journal of Instrumentation, **1**, P04002 (2006).

[7] T. Wangler, *RF Linear Accelerators*, John Wiley &. Sons, Inc., pp. 277, equation 9.40 (1998).

[8] M. Comunian et al., *Frequency map analysis of a three-dimensional particle in the core of a high intensity linac*, Physical Review Special Topics-Accelerator and beams, Vol. **4**, 124201, (2001).

[9] M. Reiser, *Theory and Design of Charged Particle Beams*, Wiley-Interscience, pp. 406 (1994).

[10] J.-P. Carneiro, *Benchmarking of Simulation Codes TRACK (ANL) and ASTRA (DESY) for the FNAL High-Intensity Proton Source*, Proceedings of Linear Accelerator Conference, Knoxville, Tennessee (2006).